Light-induced absorption switching in a $Nd^{3+}:GdFe_3(BO_3)_4$ single crystal

Ph. Goldner, O. Guillot-Noël, and J. Petit*
Laboratoire de Chimie de la Matière Condensée de Paris CNRS–UMR 7574, Ecole Nationale Supérieure de Chimie de Paris 11, rue Pierre et Marie Curie, F-75005 Paris, France

M. Popova
Institute of Spectroscopy, Russian Academy of Sciences, Troitsk, Moscow Region 142190, Russia

L. Bezmaternykh
L.V. Kirensky Institute of Physics, Siberian Branch of RAS, Krasnoyarsk 660036, Russia

(Received 2 February 2007; revised manuscript received 10 May 2007; published 1 October 2007)

$Nd^{3+}:GdFe_3(BO_3)_4$ crystal is subjected to two magnetic phase transitions corresponding to a magnetic ordering and a spin reorientation. The latter occurs at 6.55 K and is observed as a sudden change in the shape of the absorbance spectra of Nd^{3+} transitions. The largest variations in the absorbance of the sample are found near 740.5 nm in one of the $^4I_{9/2} \rightarrow {}^4F_{7/2}, {}^4S_{3/2}$ transition lines. Measuring the absorption with a laser may heat the sample and induce the phase transition, resulting in a laser power dependent absorbance. When the variation of absorbance is large across the phase transition, it exhibits a switching behavior with respect to the laser power. However, this is not true when the absorbance increase is small or when the absorbance decreases across the phase transition. We explain these results by the nonlinear absorbance variations, a feedback mechanism provided by the cryostat held at a fixed temperature and a nonuniform sample temperature. These features can be taken into account by a simple one-dimensional thermal diffusion model which describes reasonably well the experiments.

DOI: 10.1103/PhysRevB.76.165102 PACS number(s): 78.40.−q, 75.30.Kz, 78.20.−e

I. INTRODUCTION

The possibility of controlling the optical properties of a system by light, without relying on external devices such as cavities, has been studied in rare-earth-doped crystals for several years. For example, bistability of Yb^{3+} luminescence has been reported in a number of crystals such as $Yb^{3+}:Cs_3Y_2Br_9$,[1] $Yb^{3+}:CsCdBr_3$,[2] $Yb^{3+}:LiNbO_3$,[3] $Yb^{3+}:YCa_4O(BO_3)_3$,[4] or $Yb^{3+}:NdPO_4$.[5] Luminescence switching under laser excitation has also been demonstrated in $Yb^{3+}:Nd_3BWO_9$.[6]

Interest in these processes has been driven by potential applications in optical communication systems or sensors but also by the unclear nature of the observed behaviors. Although intrinsic mechanisms based on interactions between two rare-earth ions or between a rare-earth ion and its environment are theoretically able to induce bistability or switching,[7,8] they have not yet been demonstrated experimentally in an unambiguous way. On the other hand, thermal effects due to the heating by the excitation laser explain at least partially several results.[3–5,9] Thermal effects can also modify the emission or absorption properties of a rare-earth ion when a phase transition is induced in the material. This has been shown, for example, in $Yb^{3+}:Sr_{0.6}Ba_{0.4}Nb_2O_6$ which exhibits a ferroelectric phase transition.[10] Rare-earth-doped crystals in which magnetic phase transitions occur have also been thoroughly studied.[11–13] These hosts are of particular interest since a strong effect on the optical properties of rare-earth ions with an odd number of electrons is observed across the phase transitions: for example, magnetic ordering induces splitting of Kramers doublets which can reach several tens wavenumbers. Moreover, in some compounds, a magnetic spin reorientation occurs as a first order phase transition. This also influences the rare-earth ion spectra which experience sudden changes in intensity and/or shape at the phase transition temperature. This gives an opportunity to observe fast and sensitive switchings of the spectroscopic properties with temperature and laser power.

Following this idea, we investigated the spectroscopic properties of a 4% Nd^{3+}-doped single crystal of $GdFe_3(BO_3)_4$. This crystal has a trigonal structure at room temperature (space group D_3^7) and incorporates chains of FeO_6 octahedra parallel to the c axis. Gadolinium ions occupy sites of D_3 symmetry between these chains. Previous studies showed that several phase transitions occur in this crystal.[14–17] First of all, a structural phase transition was observed around 156 K. Then, in a 1% Nd^{3+} doped crystal, a magnetic ordering is found around 37 K and a magnetic spin reorientation around 9 K. These magnetic transitions have been clearly observed by Nd^{3+} high-resolution optical spectroscopy using a weak intensity light beam which had a negligible heating effect.[14] In this work, we used a laser to probe the absorption of the sample and the dependence of the latter as a function of the laser power could be studied at several wavelengths. In particular, very sharp and large absorption switchings as a function of the laser power were observed for certain wavelengths and smooth variations at other wavelengths.

The paper is organized as follows. In Sec. II, the experimental apparatus is presented. In Sec. III, low-temperature spectroscopy of the sample is reported. In Sec. IV, absorbance variations as a function of the laser power are described and modeled.

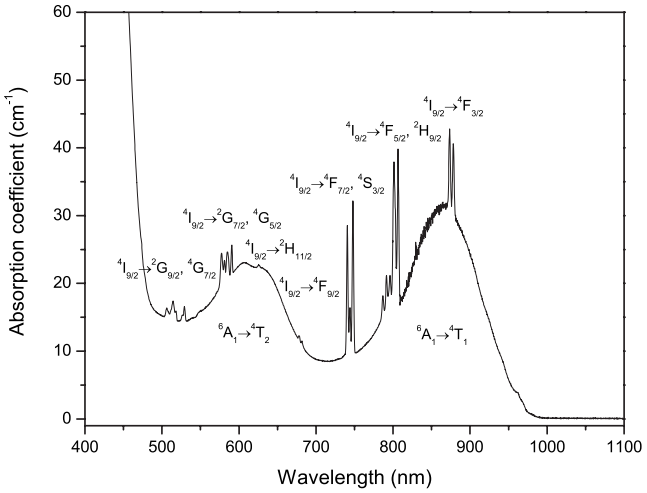

FIG. 1. Absorption spectrum of Nd^{3+}:$GdFe_3(BO_3)_4$ at 10 K. The upper (lower) labels refer to Nd^{3+} (Fe^{3+}) transitions.

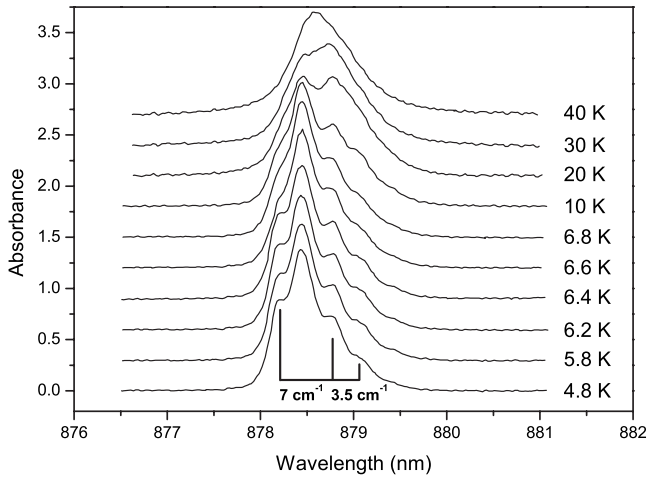

FIG. 2. Absorption spectra of the $^4I_{9/2}(0)\rightarrow{}^4F_{3/2}(0)$ transition in Nd^{3+}:$GdFe_3(BO_3)_4$ at different temperatures. The splittings of the $^4I_{9/2}(0)$ and $^4F_{3/2}(0)$ levels are indicated.

II. EXPERIMENTAL

The 4 at. % Nd^{3+}:$GdFe_3(BO_3)_4$ crystal was grown using a $K_2Mo_3O_{10}$-based flux.[18] The sample was green in color and of good optical quality. Its thickness was reduced to 360 μm and two faces were polished for optical measurements. Absorption spectra were recorded with a Varian Cary 5 spectrophotometer equipped with a Helix M22 closed-cycle helium cryostat. The halogen lamp used as the light source in this device is weak enough to prevent heating of the sample. Alternatively, an argon-pumped Ti-Sa laser (Coherent 890) was used to measure absorption around 740 and 870 nm and to vary the incident power on the sample approximately between 1 and 10 mW. One face of the sample was stuck with silver paint to a copper block inside a Janis helium vapor cryostat. The minimum temperature measured just above the copper block was 4.3 K. The laser light was incident on the other face and a small hole in the copper block allowed the beam to pass and reach a silicon photodiode. A reference arm was set up in order to measure accurately the transmission spectra. A motorized variable density filter allowed us to vary the laser power. In order to reach equilibrium before each measurement, the laser power was increased or decreased in steps of about 0.2 mW every 4 s.

III. LOW-TEMPERATURE OPTICAL SPECTROSCOPY

Figure 1 displays the absorption spectrum obtained at 10 K on the 4% Nd^{3+}:$GdFe_3(BO_3)_4$ sample using the Cary 5 spectrophotometer. Two broad bands centered at 610 and 865 nm and corresponding to Fe^{3+} transitions from the $^6A_1$ ground state are observed. The narrow Nd^{3+} transitions from the $^4I_{9/2}$ ground state are superimposed on these bands. In particular, the $^4I_{9/2}\rightarrow{}^4F_{3/2}$ transition at 875 nm is very close to the maximum of the $^6A_1\rightarrow{}^4T_1$ band. This favors nonradiative energy transfer from Nd^{3+} to Fe^{3+} and may explain that no emission from the $^4F_{3/2}$ level was observed in this compound. Since no emission from Fe^{3+} ions is expected because of their high concentration, we conclude that excitation of this crystal in the range 739–880 nm results mainly in heating through nonradiative relaxations. This spectrum also shows that the most intense transition of Nd^{3+}, occurring at 743 nm ($^4I_{9/2}\rightarrow{}^4F_{7/2}$,$^4S_{3/2}$), is also close to the minimal Fe^{3+} absorption. Excitation around this wavelength therefore maximizes the effect of Nd^{3+} absorption on the sample temperature with respect to Fe^{3+} ions. This will be discussed in Sec. IV.

The absorption spectra between the lowest crystal field levels of the $^4I_{9/2}$ and $^4F_{3/2}$ multiplets [denoted $^4I_{9/2}(0)\rightarrow{}^4F_{3/2}(0)$] are shown in Fig. 2 for different temperatures. These spectra were obtained using the Ti-Sa laser set at a low power (<1 mW) to avoid heating of the sample. A splitting of the line appears between 30 and 40 K and corresponds to a magnetic ordering of Fe^{3+} ions.[16] In this case, exchange interactions between Fe^{3+} and Nd^{3+} ions remove the twofold degeneracy of the Stark levels. Thus, when temperature is further decreased, four lines gradually appear. A sudden change in the spectrum occurs at 6.55 K as can be seen, for example, by recording the absorption at 878.70 nm as a function of the temperature (Fig. 3). This second phase transition, which occurs in a very small temperature range ($\leqslant$0.1 K), is of first order and corresponds to a reorientation of the Fe^{3+} spins.[14] The temperature of this second phase transition is about 2.5 K lower than in a 1% Nd^{3+}:$GdFe_3(BO_3)_4$.[14] This could be due to a larger disorder in the Gd^{3+} sublattice due to the higher Nd^{3+} doping (4 at. % vs 1 at. %). This increased disorder is confirmed by the 4.8 K spectrum (Fig. 2) in which the inhomogeneously broadened lines are significantly wider in the 4% sample compared to the 1% one. From the 4.8 K spectrum, splittings of 3.5 and 7.5 cm^{-1} were determined for the Stark splittings of the $^4F_{3/2}(0)$ and $^4I_{9/2}(0)$ levels, in agreement with Ref. 14.

We also performed absorption measurements for increasing and decreasing temperatures (Fig. 3). No hysteresis larger than the temperature step (0.2 K) was observed. However, as shown by the simulations of Sec. IV, a hysteresis of the phase transition is not necessary to observe bistability as a function of the laser power.[9]

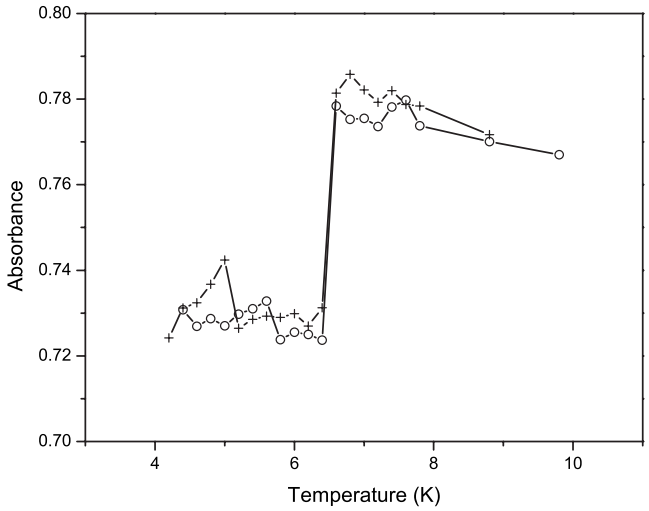

FIG. 3. Nd^{3+}:$GdFe_3(BO_3)_4$ absorption at 878.70 nm as a function of temperature [$^4I_{9/2}(0) \rightarrow {}^4F_{3/2}(0)$ transition]. Circles (crosses): increasing (decreasing) temperatures

The $^4I_{9/2} \rightarrow {}^4F_{7/2}, {}^4S_{3/2}$ optical transition occurring between 739.5 and 750 nm was also recorded with the Ti-Sa laser kept at a low power (Fig. 4). On the high-energy peak of the $^4I_{9/2} \rightarrow {}^4F_{7/2}, {}^4S_{3/2}$ transition, the magnetic ordering is observed as splittings and sudden changes in the absorption spectrum, as in the case of the $^4I_{9/2}(0) \rightarrow {}^4F_{3/2}(0)$ transition. However, much larger changes are recorded across the spin reorientation phase transition (see the inset of Fig. 4 also). The maximum factors of increase and decrease of the Nd^{3+} absorbance are, respectively, 4 at 740.30 nm and 2.2 at 740.64 nm when the temperature increases from 6.4 to 6.6 K. These wavelengths are indicated by arrows in Fig. 4 and were used for the laser induced absorption switching experiments.

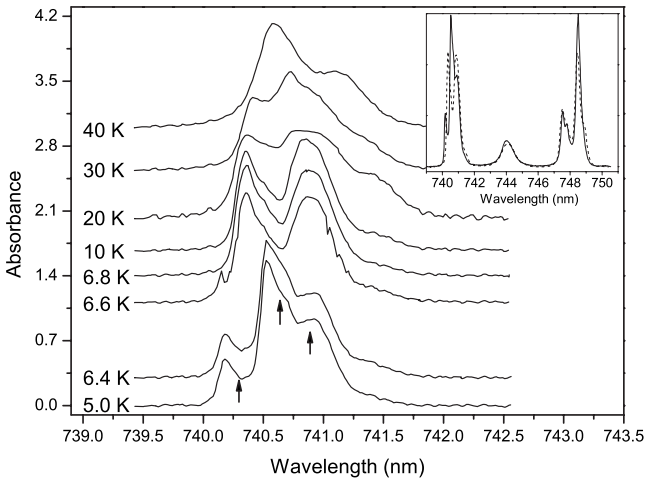

FIG. 4. Nd^{3+}:$GdFe_3(BO_3)_4$ absorption spectra of the $^4I_{9/2} \rightarrow {}^4F_{7/2}, {}^4S_{3/2}$ 740 nm transition at different temperatures. The arrows show the wavelengths used for the laser induced phase transition experiments. Inset: Complete spectrum at 4.4 (solid line) and 8 K (dashed line).

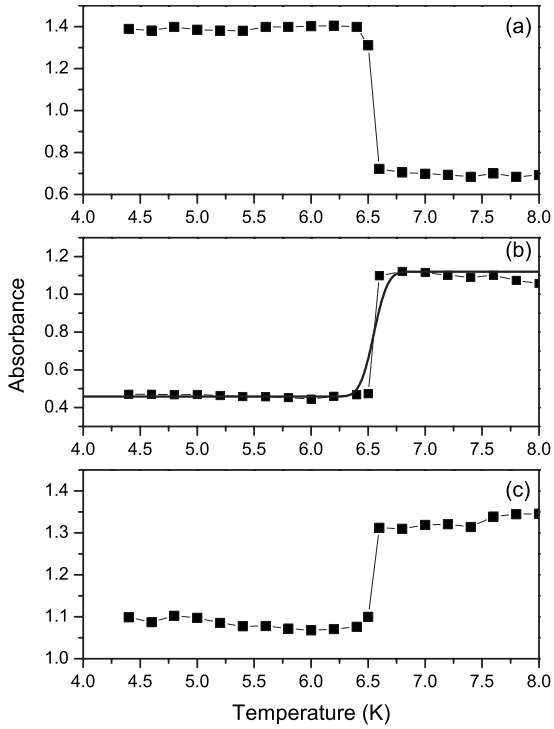

FIG. 5. Nd^{3+}:$GdFe_3(BO_3)_4$ absorption at 740.64 nm (a), 740.30 nm (b), and 740.87 nm (c) as a function of temperature. Thick line on (b) modeling of the absorption transition with an equivalent width for the phase transition of 0.49 K (see text).

IV. LIGHT-INDUCED ABSORPTION SWITCHING

For these experiments, the absorption of the Nd^{3+}:$GdFe_3(BO_3)_4$ sample was measured as a function of the increasing laser power. The copper block holding the sample was maintained at 4.5 K. The laser was set at the two wavelengths of maximal absorbance variations (740.64 and 740.30 nm) across the lowest temperature phase transition. A third wavelength, 740.87 nm, was also used in order to study the effect of a lower Nd^{3+} absorbance variation (a factor of 1.3 across the phase transition). These wavelengths are marked with arrows in Fig. 4.

The absorbances of the sample as a function of temperature and at the three wavelengths of interest were extracted from the spectra of Figs. 4 and 1 and are displayed in Fig. 5. In this figure, as well as in Figs. 6, 8, and 9, the actual absorbance of the sample is reported, which includes contributions from both Nd^{3+} and Fe^{3+} ions. As expected, a sharp variation of absorbance occurs at $T_{PT}=6.55$ K in each case. The absorbance was then measured as a function of the laser power (Fig. 6, open circles). Note that the laser powers are in arbitrary units but are consistent with each other. At 740.30 nm [Fig. 6(b)], the total absorbance suddenly increases by a factor of 2.3 over a range of $\Delta P_L/P_L < 3.3 \times 10^{-2}$, when the laser power P_L reaches 15 arb. units. However, at 740.64 and 740.87 nm, the variations of the absorbance are much slower with the laser power variation [Figs. 6(a) and 6(c)] than with the temperature [Figs. 5(a) and 5(c)].

These different behaviors contrast very clearly with the absorbance curves recorded as a function of temperature

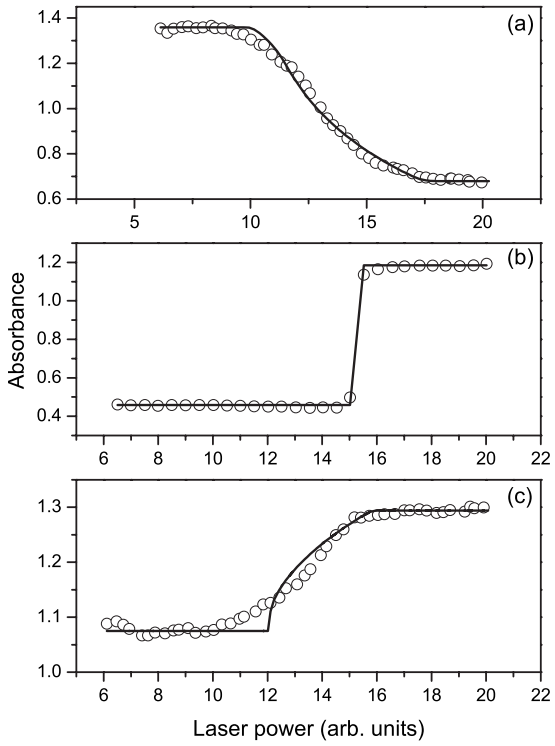

FIG. 6. Nd^{3+}:$GdFe_3(BO_3)_4$ absorption at 740.64 nm (a), 740.30 nm (b), and 740.87 nm (c) as a function of the laser power (open circles) and computed curves with an equivalent width of the phase transition of 0.091 K for the absorption transition (solid lines).

(Fig. 5) which all exhibit a sharp transition at the phase transition temperature. This indicates that the absorbance variations induced by the laser heating not only involves the nonlinear variation of absorbance across the phase transition but also a feedback process as seen, for example, in optical bistability processes.[19] The combination of the absorbance variation magnitude with the feedback can result in a switching behavior [Fig. 6(b)] or only smooth changes [Figs. 6(a) and 6(c)].

Such a mechanism, involving a nonlinear absorption change and a feedback mechanism, has been proposed to explain optical bistability based on thermal effects.[9] In this case, the feedback is provided by the cryostat which is held at a constant temperature. This produces switching behavior of the absorbance as a function of the laser power: when the sample temperature reaches a point where the absorbance increases rapidly with the temperature, a large amount of heat is generated by the laser absorption. To dissipate this heat, the sample temperature has to increase in order to increase the cooling provided by the cryostat. This further increases the absorbance and therefore the absorbed laser power and the sample temperature. Finally, the equilibrium is reached at a temperature significantly higher than the initial one. This is observed as a switching in the sample absorbance.

This mechanism can be modeled in the following way. The cooling rate R_c due to the cryostat is equal to

$$R_c = \beta(T_S - T_c), \tag{1}$$

where β describes the heat transfer to the copper block and T_c (T_S) are the copper (sample) temperatures. This cooling rate is equal to the heating rate R_h provided by the laser which is proportional to the incident laser power P_L:

$$R_h = (1 - e^{-\alpha l})P_L = KP_L, \tag{2}$$

where α is the absorption coefficient and l is the thickness of the sample. KP_L is therefore the absorbed power which is assumed to be entirely dissipated in the crystal in a nonradiative way because of the lack of emission in this material. A partially radiative decay could be taken into account by replacing K by $(1-\eta)K$, where η is the global radiative efficiency of the sample. However, this has no effect on the following discussions and modelings, since it is equivalent to a scaling factor on the laser power. With the steady state condition $R_c = R_h$, we deduce the relation between small variations in sample temperature and absorbed power around a state (T_S, K, P) of the sample

$$\frac{\Delta T_S}{T_S - T_c} = \frac{\Delta K}{K} + \frac{\Delta P_L}{P_L}. \tag{3}$$

Starting from a sample state below the phase transition temperature T_{PT}, the laser power is increased until T_S is equal to T_{PT}. From this state, Eq. (3) allows us to determine a value of ΔP_L which will produce an increase of the sample temperature ΔT_S larger than the phase transition temperature range ΔT_{PT}: when ΔK is positive across the phase transition, $\Delta T_S \geqslant \Delta T_{PT}$ is obtained for $\frac{\Delta P_L}{P_L} \geqslant \frac{\Delta T_{PT}}{T_{PT}-T_c}$ and if K decreases across the phase transition, $\Delta T_S \geqslant \Delta T_{PT}$ corresponds to $\frac{\Delta P_L}{P_L} \geqslant \frac{\Delta T_{PT}}{T_{PT}-T_c} - \frac{\Delta K}{K}$.

In the three absorbances vs temperature shown in Fig. 5, the phase transition occurs on a range of at most 0.1 K around 6.55 K, giving a maximal relative variation $\frac{\Delta T_{PT}}{T_{PT}-T_c}$ of 5×10^{-2} for $T_c = 4.5$ K. In the case of the transmission at 740.3 nm [Fig. 6(b)], $\Delta K > 0$ across the phase transition, which indicates that $\frac{\Delta P_L}{P_L} \geqslant 5\times10^{-2}$ will be enough to change the sample magnetic phase. In agreement, the sudden increase of absorbance when the laser power exceeds about 15 arb. units in Fig. 6(b) gives $\frac{\Delta P_L}{P_L} = 3.3\times10^{-2}$. At 740.87 nm, we also have $\Delta K > 0$ across the phase transition [Fig. 5(c)] and the same conclusion holds: just before the phase transition, a relative increase of the laser power of 5×10^{-2} should be able to increase the sample temperature over T_{PT}. However, the recorded variation of absorbance with the laser power is smooth and extends on 5.4 arb. units around an average value of 12.5 leading to $\frac{\Delta P_L}{P_L} = 0.43$ which is nearly 10 times $\frac{\Delta T_{PT}}{T_{PT}-T_c}$. At 740.64 nm [Fig. 5(a)], $\frac{\Delta K}{K} = -0.16$ across the phase transition, so that the relative variation in laser power necessary to increase the temperature over T_{PT} should be ≈ 0.21. In opposition, we observed again a smooth change corresponding to $\frac{\Delta P_L}{P_L} = 0.62$.

The discrepancy between our results and the heat exchange model can be traced back to a feedback which is too efficient and always results in a switching. To explain the

smooth changes observed, we propose to take into account the temperature gradient in the sample due to its finite thermal conductivity. In this case, the heating produced by the laser absorption when one part of the sample reaches the phase transition temperature will still be compensated by an increase in the sample temperature. However, the temperature gradient will also be conserved and if the amount of heat generated by the laser is not too large, only part of the sample will experience the phase transition. The increase in absorbance will then be smaller than what is observed when the whole sample experiences the phase transition as in the experiments where the temperature is varied. Further increase of the laser power will move the boundary between parts of the sample under and over T_{PT}. How this boundary moves with the laser power will depend not only on the phase transition characteristics but also on the thermal conductivity of the crystal, the transfer coefficient to the copper block, and the geometric details of the system. These additional parameters can result in a phase transition border moving slowly in the crystal as a function of the laser power. A complete simulation of the sample temperature is difficult: the thermal parameters are unknown, especially at very low temperatures; the geometry is complex since the laser escapes by a hole through the copper block; the laser intensity has a Gaussian transverse profile. Instead of introducing many fitting parameters, we have tried to reproduce our experiments with a 1D model in a semi-quantitative way. This model assumes that the thermal exchanges occur only with the copper block, because the exchange with the helium gas should be much lower. The equations to solve in the steady state regime reduce to

$$\frac{dT_S}{dt} = 0 = k\frac{d^2T_S}{dx^2} + \alpha(x)I_L(x), \tag{4}$$

$$k\frac{dT_S}{dx}(l) = h[T_S(l) - T_c], \tag{5}$$

$$k\frac{dT_S}{dx}(0) \approx 0, \tag{6}$$

where x is the distance from the entrance face of the sample, I_L is the laser intensity, k the crystal thermal conductivity, and h the thermal transfer coefficient between the crystal and the copper block. Since I_L, which is proportional to P_L, is in arbitrary units, a fit of the experimental points by the model is only able to determine the ratios k/h and $I_L(0)/h$.

For a given laser power, the crystal temperatures were calculated using a simultaneous overrelaxation algorithm[20] implemented under MATLAB software. To avoid instabilities in the computations, the temperature dependence of the absorption coefficient α was modeled by an error function

$$\alpha(T_S) = \frac{\alpha_{\mathrm{HT}} - \alpha_{\mathrm{LT}}}{2}\,\mathrm{erf}\left(\frac{3.642(T_S - T_{PT})}{\Delta T_e}\right) + \frac{\alpha_{\mathrm{HT}} + \alpha_{\mathrm{LT}}}{2}, \tag{7}$$

where α_{LT} (α_{HT}) is the absorption coefficient under (over) the phase transition. The effective temperature width of the transition ΔT_e is defined so that $\alpha(T_{PT}-\Delta T_e/2)=0.99\alpha_{\mathrm{LT}}$ and $\alpha(T_{PT}+\Delta T_e/2)=0.99\alpha_{\mathrm{HT}}$. The same value of ΔT_e is used in the fit for the three different wavelengths. Once a temperature profile was determined, it was used as the starting profile for the computation at the next laser power. This was done in order to reproduce more accurately the experimental conditions and especially the experiments where the laser power is first increased and then decreased (see below). For the computation of the first temperature profile, corresponding to a low laser power, we started from a uniform temperature of 4.5 K.

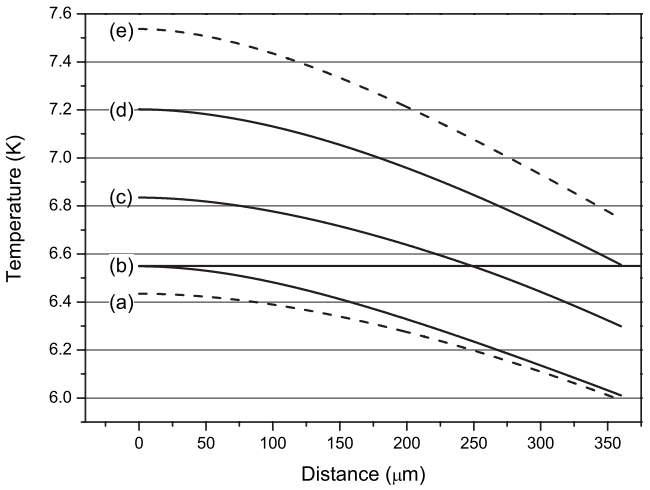

FIG. 7. Temperature in the $Nd^{3+}:GdFe_3(BO_3)_4$ sample as a function of the distance from the input face. (b),(c),(d) laser wavelength: 740.64 nm, laser power: 10.5,13,17.5 (arb. units). (a),(e) laser wavelength: 740.3 nm, laser power: 15.5, 15.6 (arb. units). Thick horizontal line: phase transition temperature.

We first set $\Delta T_e=0.091$ K to reproduce the curves of absorbance versus temperature of Fig. 5. The experimental points of absorbance versus laser power were fitted simultaneously with k/h and $I_{L,i}(0)/h$ as free parameters, where i corresponds to one of experimental data sets (a), (b), or (c) in Fig. 6. The three $I_{L,i}(0)/h$ parameters were set free to allow for small variations in the laser setup from one experiment to the other. The fit resulted in $k/h=7.1\times10^{-4}$ and in $I_L(0)/h$ values which differed by ±6.4% from their mean value. Although the computed curves reproduce reasonably well the experiments at 740.64 and 740.30 nm [Figs. 6(a) and 6(b)], the agreement is worse at 740.87 nm [Fig. 6(c)]. In this case, the computed absorbance increases still too fast with the laser power. This could be due to the smaller absorbance difference across the phase transition at this wavelength (a factor of 1.2 for the total absorbance compared to 2.3 and 2 at 740.30 and 740.64 nm, respectively): transverse temperature gradients not taken into account in the 1D model could be more important here.

The computed temperatures along the thickness of the sample are shown in Fig. 7. All curves are similar with a zero slope at the $x=0$ position, fixed by the corresponding boundary condition, and a smooth decrease toward the end of the sample attached to the copper block. At 740.64 nm [curves (b), (c), and (d)], the phase transition position moves inside

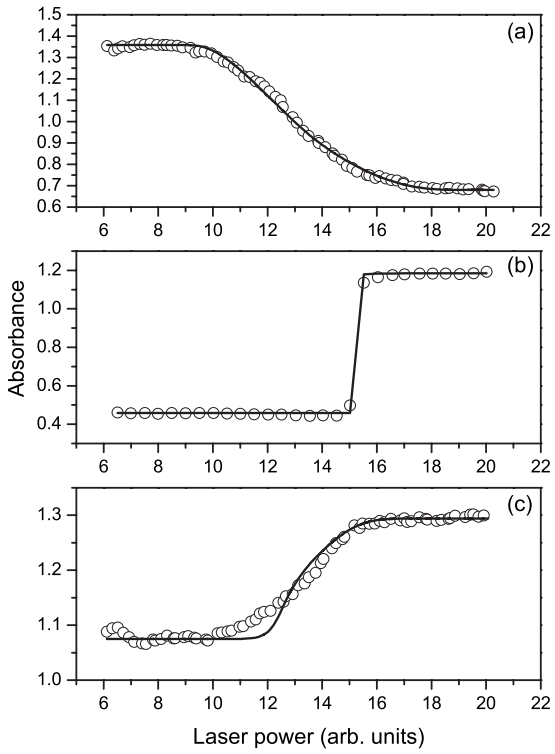

FIG. 8. $Nd^{3+}:GdFe_3(BO_3)_4$ absorption at 740.64 nm (a), 740.30 nm (b), and 740.87 nm (c) as a function of the laser power (open circles) and computed curves with an equivalent width of the phase transition of 0.49 K for the absorption transition (solid lines).

the sample when the laser power increases from 10.5 to 17.5 (arb. units). This is in agreement with the proposed origin of the smooth variation of the absorbance with the laser power. On the other hand, at 740.30 nm, the sample is entirely in the low-temperature phase until $P_L=15.5$ arb. units and suddenly entirely in the high-temperature phase for $P_L \geqslant 15.6$. In this case, the feedback mechanism is very efficient and the range of laser power in which the sample shows two phases is extremely reduced. This results in a large and sudden absorbance increase with increasing laser power. It can also be seen that the temperature gradient is around 0.2 K for a distance of 100 μm in the middle of the sample for the different curves. Since the laser beam waist was ≈ 50 μm, this suggests that the transverse Gaussian profile of the laser intensity could indeed induce significant temperature gradients which could in turn induce phase transitions.

In an attempt to better reproduce the experiments, another fit to the experimental data was performed with the effective width of the phase transition [i.e., ΔT_e in Eq. (7)] set as an additional free parameter (but identical for the three wavelengths). The calculated curves are shown in Fig. 8 and are clearly closer to the experimental data, especially for curves (a) and (c). The root-mean-square deviation is reduced from the previous case ($\Delta_e=0.091$ K) by 34% with best fit parameters of $k/h=8.56\times 10^{-4}$ and variations in $I_L(0)/h$ of $\pm 6\%$. The best fit effective width parameter is, however, significantly larger than the experimental one: $\Delta T_e=0.49$ K [see Fig. 5(b)]. This shows that the temperature gradients not included in the 1D model can be partially taken into account by a smoother phase transition.

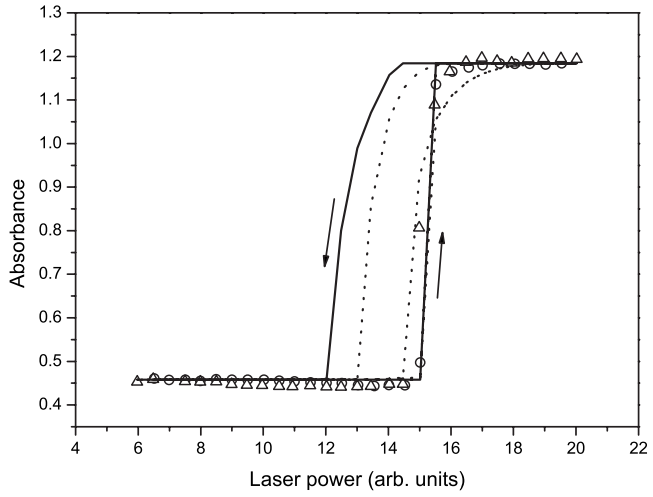

FIG. 9. $Nd^{3+}:GdFe_3(BO_3)_4$ absorption at 740.3 nm as a function of the laser power. Triangles (circles): increasing (decreasing) power; solid (dotted) line: computed curve for increasing and decreasing laser powers $\Delta T_e=0.091$ K ($\Delta T_e=0.49$ K).

Finally, we investigated the possibility of a bistability of the absorbance versus the laser power in this system. The laser power was first increased from a low power so that the sample maximal temperature was well below the phase transition to one where the minimal sample temperature was well above the phase transition and then decreased again. Such an experiment for the transition at 740.30 nm is presented in Fig. 9. No hysteresis was observed with the given laser power fluctuations which limited the minimum step for power variations to 0.5 arb. units. Using the parameters of the two previous fits (with $\Delta T_e=0.091$ and 0.49 K), we also computed the same cycle by the 1D model (Fig. 9, solid and dotted lines). In both cases, a hysteresis cycle is predicted with a larger opening for the smaller effective width of the phase transition. The hysteresis cycle is also predicted by the model of Eqs. (1) and (2): the strong nonlinearity of the absorbance with temperature and the feedback provided by the cryostat result in a large increase in temperature as soon as the sample temperature is above T_{PT}. From this point, if the laser power in decreased, the sample temperature will first smoothly decrease to T_{PT}, because the absorption coefficient is nearly constant in this region. Once the sample is at T_{PT}, a small decrease in the laser power will induce a large drop in temperature, again because of the sudden decrease of absorbance and the feedback mechanism. A hysteresis cycle should therefore be observed and the negative experimental result points again to 2D or 3D effects that tend to produce smooth phase changes in the sample. This effect can be partially taken into account in the 1D model by increasing the effective phase transition width and simulations show that the cycle disappears for $\Delta T_e \geqslant 1.46$ K.

V. CONCLUSION

The low-temperature absorption spectrum of a $4\%\,Nd^{3+}:GdFe_3(BO_3)_4$ single crystal shows sharp lines of Nd^{3+} superimposed on large bands due to Fe^{3+} ions. No lu-

minescence could be recorded from the sample upon excitation between 739 and 880 nm, probably because of nonradiative energy transfers from Nd^{3+} to Fe^{3+} and the concentration quenching of the latter. The two magnetic phase transitions occurring in this compound were observed on Nd^{3+} absorption spectra which exhibited sudden changes in shape across the phase transition located at the lowest temperature (6.55 K). No hysteresis was found on the variations of absorbance as a function of temperature across this phase transition. Using a laser of moderate power ($\approx$10 mW), we showed that the low-temperature phase transition can be induced by the heating due to the laser light. This effect was investigated in detail on one line of the $^4I_{9/2} \rightarrow {}^4F_{7/2}, {}^4S_{3/2}$ transition which gave the most important changes in absorbance at the phase transition. The complex modifications of the line shape across the phase transition allowed us to study three cases: a large increase, a large decrease, and a small increase in absorbance with increasing temperature. In the first case, the absorbance variation induced by the laser is very sudden resulting in a switching behavior. However, in the two other cases, the absorbance varies smoothly with the laser power. This can be explained by taking into account the feedback provided by the cryostat and the nonuniform sample temperature in addition to the nonlinear absorbance variations. These circumstances result in a phase transition boundary which moves inside the sample as a function of the laser power. A simple 1D thermal diffusion model reproduces reasonably well the experimental results but the phase transition temperature range has to be significantly increased compared to experiments. These discrepancies are attributed to the transverse intensity profile of the laser beam and 2D or 3D geometric features. Although no bistability of the absorbance versus laser power was observed, as could have been expected from the model predictions, the observed switching phenomenon itself is of interest when considering a possibility to control the optical properties of a system by light.

ACKNOWLEDGMENTS

This work was partially supported by the CNRS-RAS exchange program. M.P. and L.B. acknowledge support from the Russian Foundation for Basic Research under Grants Nos. 07-02-01185a and 06-02-16255a and from the Russian Academy of Sciences under the Programs for Basic Research.

*Present address: ONERA, Département des Matériaux et Systèmes Composites, 29, Avenue de la Division Leclerc, Boîte Postal 72, 92322 Châtillon Cedex, France.

[1] M. Hehlen, H. Güdel, Q. Shu, and S. Rand, J. Chem. Phys. **104**, 1232 (1996).
[2] M. P. Hehlen, A. Kuditcher, S. C. Rand, and S. R. Lüthi, Phys. Rev. Lett. **82**, 3050 (1999).
[3] M. Ramírez and L. Bausá, J. Lumin. **102-103**, 206 (2003).
[4] Ph. Goldner, O. Guillot-Noël, and P. Higel, Opt. Mater. **26**, 281 (2004).
[5] A. Rodenas, D. Jaque, J. Garcia Sole, A. Speghini, M. Bettinelli, and E. Cavalli, Phys. Rev. B **74**, 035106 (2006).
[6] D. Jaque, J. G. Sole, L. Macalik, J. Hanuza, and A. Majchrowski, Appl. Phys. Lett. **86**, 011920 (2005).
[7] O. Guillot-Noël, L. Binet, and D. Gourier, Phys. Rev. B **65**, 245101 (2002).
[8] O. Guillot-Noël, Ph. Goldner, and D. Gourier, Phys. Rev. A **66**, 063813 (2002).
[9] D. Gamelin, S. Lüthi, and H. Güdel, J. Phys. Chem. B **104**, 11045 (2000).
[10] M. O. Ramirez, L. E. Bausa, A. Speghini, M. Bettinelli, L. Ivleva, and J. Garcia Sole, Phys. Rev. B **73**, 035119 (2006).
[11] M. N. Popova, J. Alloys Compd. **275-277**, 142 (1998).
[12] M. N. Popova, S. A. Klimin, E. P. Chukalina, E. A. Romanov, B. Z. Malkin, E. Antic-Fidancev, B. V. Mill, and G. Dhalenne, Phys. Rev. B **71**, 024414 (2005).
[13] N. P. Kolmakova, S. V. Koptsik, G. S. Krinchik, and A. Y. Sarantsev, J. Magn. Magn. Mater. **131**, 253 (1994).
[14] R. Z. Levitin, E. A. Popova, R. M. Chtsherbov, A. N. Vasiliev, M. N. Popova, E. P. Chukalina, S. A. Klimin, P. H. M. van Loosdrecht, D. Fausti, and L. N. Bezmaternykh, JETP Lett. **79**, 423 (2004).
[15] A. I. Pankrats, G. A. Petrakovskii, L. Bezmaternykh, and O. A. Bayukov, JETP **99**, 766 (2004).
[16] E. P. Chukalina and L. N. Bezmaternykh, Phys. Solid State **47**, 1528 (2005).
[17] D. Fausti, A. A. Nugroho, P. H. M. van Loosdrecht, S. A. Klimin, M. N. Popova, and L. N. Bezmaternykh, Phys. Rev. B **74**, 024403 (2006).
[18] L. N. Bezmaternykh, V. L. Temerov, I. A. Gudim, and N. A. Stolbovaya, Crystallogr. Rep. **50**, S97 (2005).
[19] E. Abraham and S. D. Smith, Rep. Prog. Phys. **45**, 138 (1982).
[20] W. H. Press, B. P. Flannery, S. A. Teukolsky, and W. Vetterling, *Numerical Recipes in C: The Art of Scientific Computing*, 2nd ed. (Cambridge University Press, Cambridge, 2002).